

When are the $q/3$ fractional quantum Hall states stable?

Yang Liu, J. Shabani, and M. Shayegan

Department of Electrical Engineering, Princeton University, Princeton, New Jersey 08544

(Dated: January 22, 2023)

Measurements in a wide GaAs quantum well in which we can tune the Fermi energy (E_F) to lie in different Landau levels (LLs) of two electric subbands reveal a remarkable pattern for the appearance and disappearance of fractional quantum Hall states at $\nu = 10/3, 11/3, 13/3, 14/3, 16/3,$ and $17/3$. The data provide direct evidence that the $q/3$ states are stable and strong even at such high fillings as long as E_F lies in a ground-state ($N = 0$) LL of either of the two electric subbands. Moreover, the states remain stable very near the crossing of two LLs belonging to the two subbands, especially if the levels have parallel spins.

The fractional quantum Hall (FQH) effect [1], signaled by the vanishing of the longitudinal resistance and the quantization of the Hall resistance, is the hallmark of an interacting two-dimensional electron system (2DES) in a large perpendicular magnetic field. It is a unique incompressible quantum liquid phase described by the celebrated Laughlin wavefunction [2]. In a standard, single-subband 2DES confined to a low-disorder GaAs quantum well, the FQH effect is most prominently observed at low Landau level (LL) filling factors $\nu < 2$, where the Fermi energy (E_F) lies in the spin-resolved LLs with the lowest orbital index ($N = 0$), and is conspicuously absent for $\nu > 4$ [3]. The strongest states are seen at $q/3$ fractional fillings, namely at $\nu = 1/3, 2/3, 4/3,$ and $5/3$. In contrast, when E_F lies in the second ($N = 1$) set of LLs ($2 < \nu < 4$), the equivalent $q/3$ states at $\nu = 7/3, 8/3, 10/3,$ and $11/3$ are much weaker [4, 5]. In yet higher LLs ($\nu > 4$), e.g., at $\nu = 13/3, 14/3, 16/3,$ and $17/3$, which correspond to E_F being in the third ($N = 2$) set of LLs, the FQH states are essentially absent [6–8]. This absence is believed to be a result of the larger extent of the electron wavefunction (in the 2D plane) and its extra nodes that modify the (exchange-correlation) interaction effects and favor the stability of various non-uniform charge density states (e.g., stripe phases) over the FQH states [9–13].

Here we examine the stability of the FQH states at high fillings in a 2DES where the electrons occupy two electric subbands. Our sample, grown by molecular beam epitaxy, is a 56 nm-wide GaAs quantum well (QW) bounded on each side by undoped $\text{Al}_{0.24}\text{Ga}_{0.76}\text{As}$ spacer layers and Si δ -doped layers. We fitted the sample with an evaporated Ti/Au front-gate and an In back-gate to change the 2D electron density, n , and tune the charge distribution symmetry and the occupancy of the two electric subbands. This tunability, combined with the very high mobility ($\sim 400 \text{ m}^2/\text{Vs}$) of the sample, is key to our success in probing the strength of the $q/3$ states at high fillings. We made measurements in a dilution refrigerator at a temperature of $\sim 60 \text{ mK}$.

When the QW in our experiments is "balanced", i.e., the charge distribution is symmetric, the occupied subbands are the symmetric (S) and anti-symmetric (A)

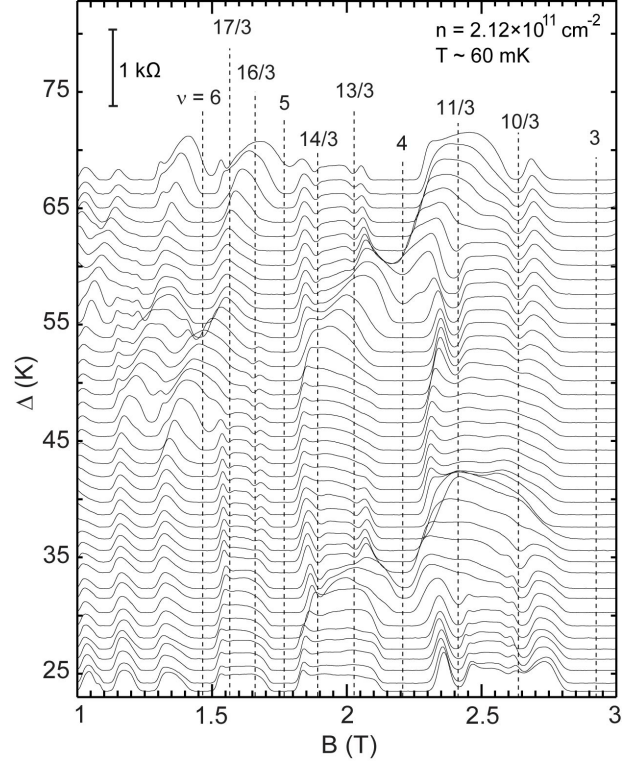


FIG. 1. Waterfall plot of R_{xx} vs. B taken at a fixed density $n = 2.12 \times 10^{11} \text{ cm}^{-2}$ as the subband separation (Δ) is increased. The scale for R_{xx} is indicated in the upper left (0 to 1 k Ω). Each trace is shifted vertically so that its zero (of R_{xx}) is aligned with its measured value of Δ which is used as the y-axis of the waterfall plot. Vertical lines mark the field positions of the filling factors, ν .

states. When the QW is "imbalanced," the two occupied subbands are no longer symmetric or anti-symmetric; nevertheless, for brevity, we still refer to these as S (ground state) and A (excited state). In our experiments, we carefully control the electron density and charge distribution symmetry in the QW via applying back- and front-gate biases [14, 15]. For each pair of gate biases, we measure the occupied subband electron densities from the Fourier transforms of the low-field ($B \leq 0.5 \text{ T}$) Shubnikov-de Haas oscillations. These Fourier trans-

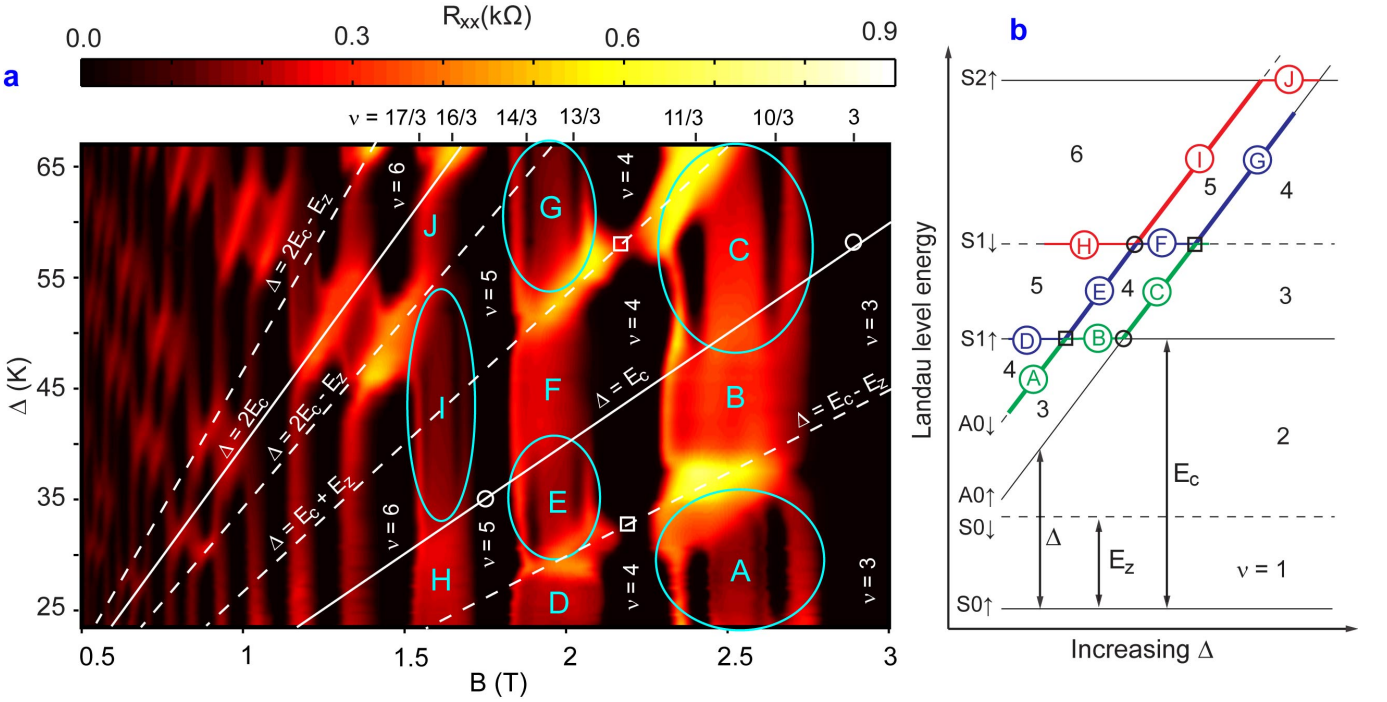


FIG. 2. Evolution of magneto-transport (R_{xx}) data taken at a fixed density $n = 2.12 \times 10^{11} \text{cm}^{-2}$ as the subband separation (Δ) is increased. (a) : A color-scale plot of the data shown in Fig. 1. The dark regions are where the integer or fractional quantum Hall states are observed, as indicated by the values of ν . The solid white lines denote $\Delta = E_C$ and $\Delta = 2E_C$, where E_C is the cyclotron energy. The white dashed lines are drawn such that they pass through the even-filling coincidences (see text). The cyan ellipses mark different regions (A, C, E, G, and I) where FQH states are observed. (b) : Schematic Zeeman Landau level diagram as a function of increasing Δ . The relevant energies, Δ , the cyclotron energy (E_C), and the Zeeman energy (E_Z), are shown. The position of the Fermi level is plotted in different colors for several filling factor regions: $3 < \nu < 4$ (green), $4 < \nu < 5$ (blue), and $5 < \nu < 6$ (red). The letters correspond to the regions in the (a) panel; the regions where fractional quantum Hall states are observed are marked by thicker lines.

forms exhibit two peaks whose frequencies, multiplied by $2e/h$, give the subband densities, n_1 and n_2 ; see, e.g., Fig. 1 in Ref. [15]. The difference between these densities directly gives the subband separation, Δ , through $\Delta = \frac{\pi \hbar^2}{m^*} (n_1 - n_2)$, where m^* is the electron effective mass. Note that, at a fixed total density, Δ is smallest when the charge distribution is balanced and it increases as the QW is imbalanced.

Figure 1 shows a series of longitudinal resistance (R_{xx}) vs. magnetic field (B) traces taken at a fixed density $n = 2.12 \times 10^{11} \text{cm}^{-2}$ as the subband spacing is increased. The y-axis is Δ , which is measured from the low-field oscillations of each trace. The same data are interpolated and presented in a color plot in Fig. 2(a).

In Figs. 1 and 2(a), we observe numerous LL coincidences at various integer filling factors, signaled by a weakening or disappearance of the R_{xx} minimum. For example, the R_{xx} minimum at $\nu = 4$ is strong and wide at all values of Δ except near $\Delta = 32$ and 58 K, marked by squares in Fig. 2a, where it becomes narrow or disappears. Such coincidences can be easily explained in a simple fan diagram of the LL energies in our system as a function of increasing Δ , as schematically shown in

Fig. 2(b). In this figure, we denote an energy level by its subband index (S or A), LL index ($N = 0, 1, 2, \dots$), and spin (\uparrow or \downarrow). Also indicated in Fig. 2(b) are the separations between various levels: the cyclotron energy ($E_C = \hbar e B / m^*$), Zeeman energy ($E_Z = g^* \mu_B B$, where g^* is the effective Landé g-factor), and Δ . From Fig. 2(b) it is clear that the condition for observing a LL coincidence at odd fillings is $\Delta = iE_C$, while for coincidences at even fillings, the condition is $\Delta = iE_C \pm E_Z$; in both cases, i is a positive integer. In Figs. 2a and 2(b), we have indicated the two coincidences at $\nu = 4$ with squares. Note that the coincidences at even fillings correspond to a crossing of two levels with antiparallel spins. In Figs. 1 and 2(a), the coincidences at low, odd fillings (e.g., $\nu = 3$ and 5) are not as easy to see at low temperatures since the resistance minima remain strong as the two LLs, which have parallel spins, cross. Such behavior has been reported previously and has been interpreted as a signature of easy-plane ferromagnetism [16, 17]. We note that our data taken at higher temperatures ($T = 0.31$ K) reveal a clear weakening of the resistance minima at odd fillings at the expected LL crossings. For example, we observe a weakening of the $\nu = 5$ minimum at $\Delta = 35$ K, and of

the $\nu = 3$ minimum at $\Delta = 58$ K; these are marked by circles in Fig. 2a, and are indeed very close to the values of E_C at the field positions of $\nu = 5$ and 3, respectively (see below).

In Fig. 2(a) we include two solid white lines representing $\Delta = E_C$ and $\Delta = 2E_C$, assuming GaAs band effective mass of $m^* = 0.067$ (in units of free electron mass). These lines indeed pass through the positions of the observed LL coincidences for odd fillings, indicating that Δ is not re-normalized in the field range of our study. In Fig. 2(a), the dashed lines represent $\Delta = iE_C \pm E_Z$, $i = 1, 2$, where g^* is chosen as a fitting parameter so that these lines pass through the even filling coincidences. We find g^* ranging from 7 to 9, implying an ~ 18 times enhancement of g^* over the GaAs band g -factor (0.44). A similarly large enhancement of g^* has been reported previously for a 2DES in a wide GaAs QW [16].

We now focus on the main finding of our work, namely the correspondence between the stability of the FQH states and the position of E_F . Note in Figs. 1 and 2(a) that FQH states are observed only in certain ranges of Δ . For example, the $\nu = 10/3$ and $11/3$ states are seen in the regions marked by A and C in Fig. 2(a) but they are essentially absent in the B region. The $\nu = 13/3$ and $14/3$ states, on the other hand, are absent in regions D and F while they are clearly seen in regions E and G.

To understand this behavior, in the fan diagram of Fig. 2(b) we have highlighted the position of E_F as a function of Δ for different filling factors by color-coded lines. Concentrating on the range $3 < \nu < 4$ (green line in Fig. 2(b), at small values of Δ (region A), E_F lies in the $A0\downarrow$ level. At higher Δ , past the first $\nu = 4$ coincidence which occurs when $\Delta = E_C - E_Z$, E_F is in the $S1\uparrow$ level (region B). Once Δ exceeds E_C , E_F lies in the $A0\uparrow$ level (region C) until the second $\nu = 4$ coincidence occurs when $\Delta = E_C + E_Z$. Note in Fig. 2(a) that strong FQH states at $\nu = 10/3$ and $11/3$ are seen in regions A and C. From the fan diagram of Fig. 2(b) it is clear that in these regions E_F is in the *ground-state* ($N = 0$) LLs of the asymmetric subband, i.e., $A0\uparrow$ and $A0\downarrow$. In contrast, in region B, where the $10/3$ and $11/3$ states are essentially absent, E_F lies in an *excited* ($N = 1$) LL, namely, $S1\uparrow$. We conclude that the $10/3$ and $11/3$ FQH states are stable and strong when E_F lies in a ground-state LL.

The data in the range $4 < \nu < 5$ corroborate the above conclusion. In Fig. 2(b) we represent the position of E_F in this filling range by a blue line. In regions E and G, E_F lies in the ground-state LLs of the asymmetric subband ($A0\downarrow$ and $A0\uparrow$), and these regions are indeed where the $\nu = 13/3$ and $14/3$ FQH states are seen. In regions D and F, on the other hand, E_F is in the excited LLs of the symmetric subband ($S1\uparrow$ and $S1\downarrow$), and the $13/3$ and $14/3$ FQH states are absent. Data at yet higher fillings ($5 < \nu < 6$) follow the same trend: FQH states at $\nu = 16/3$ and $17/3$ are seen in region I when E_F is in the

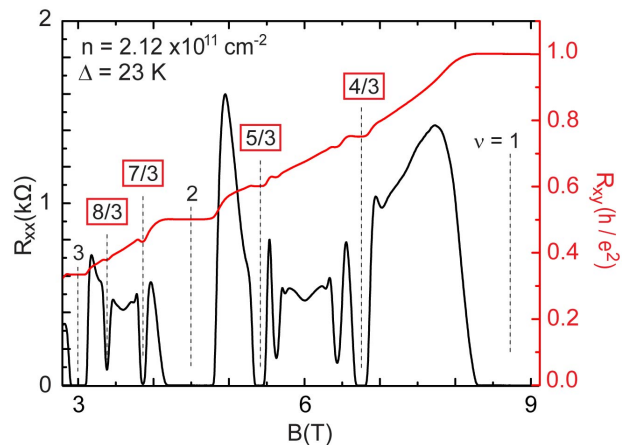


FIG. 3. Longitudinal (R_{xx}) and Hall (R_{xy}) resistances at high magnetic fields. Fractional quantum Hall states at $\nu = 4/3, 5/3, 7/3$, and $8/3$ can be clearly seen.

$A0\downarrow$ level, but they are absent in regions H or J where E_F lies in the $S1\downarrow$ or $S2\uparrow$ levels.

Next we address the FQH states observed at lower ν in our sample. Data are shown for the "balanced" QW ($\Delta = 23$ K) in Fig. 3; the R_{xx} trace is an extension of the lowest trace shown in Fig. 1. In the range $1 < \nu < 3$, strong FQH states are seen at $\nu = 4/3, 5/3, 7/3$ and $8/3$. Data taken at higher magnetic fields (not shown) reveal the presence of a very strong FQH state at $\nu = 2/3$. From the fan diagram of Fig. 2b, it is clear that E_F at these fillings lies in an $N = 0$ LL, namely, the $A0\uparrow$ ($\nu = 7/3$ and $8/3$), $S0\downarrow$ ($\nu = 4/3$ and $5/3$), or $S0\uparrow$ ($\nu = 2/3$) levels [18]. These observations are again consistent with the notion that strong $q/3$ FQH states are observed when E_F is in a ground-state LL.

Our data also allow us to assess the stability of the FQH states as two LLs approach each other. In Fig. 2a the dashed line denoted $E_C - E_Z$ marks the position of the expected crossing between the $A0\downarrow$ and the $S1\uparrow$ levels, based on the LL coincidence we observe for the $\nu = 4$ quantum Hall state. It is clear in Fig. 2a that as we approach this line from the A region, the $10/3$ and $11/3$ FQH states disappear when Δ is about 5 K away from $E_C - E_Z$. A similar statement can be made regarding the stability of the $11/3$ state as the $E_C + E_Z$ dashed line is approached from the C region, and the stability of the $13/3$ and $14/3$ states as one approaches the $E_C + E_Z$ line from the G region or the $E_C - E_Z$ line from the E region [19]. Note that what is common to all these observations is that the boundaries marked by the dashed lines correspond to the crossing of two LLs with *antiparallel* spins.

Data of Fig. 2a suggest that, when the two approaching LLs have parallel spins, the $q/3$ states remain stable even closer to the expected LL crossings. For example, the $10/3$ and $11/3$ FQH states in region C are stable very

close to the boundary (the line marked E_C) separating this region from B. Similarly, the 13/3 and 14/3 states are stable in region E close to the E_C line separating E from F. Note that in both cases, i.e., traversing from C to B or from E to F, the two approaching LLs have parallel spins (see Fig. 2b). We conclude that the relative spins of the two approaching LLs also play a role in the stability of the $q/3$ FQH states. It is worth emphasizing that, as is evident from Figs. 1 and 2a data, the relative spins of the two approaching LLs also play a crucial role in the stability of the *integer* quantum Hall (IQH) states. For antiparallel-spin LLs, the IQH state (e.g., at $\nu = 4$) becomes very weak or completely disappears, while for the parallel-spin LLs the IQH state (e.g., at $\nu = 3$), remains strong. This behavior has been attributed to easy-axis (for an opposite-spin crossing) and easy-plane (for a same-spin crossing) ferromagnetism [16, 17, 20]. We add that the stability we observe for the $q/3$ FQH states near the LL crossings implies that the mixing of LLs (belonging to two different subbands) is not playing an important role in de-stabilizing these states.

We highlight three further observations. First, strong FQH states at large, $q/3$ fillings have been recently observed in very high quality graphene samples [21]. These qualitatively resemble what we see in our two-subband system. It is tempting to associate the valley degree of freedom in graphene with the subband degree of freedom in our sample. But the LL structure in graphene is of course different from GaAs so it is not obvious if this association is valid. Second, data taken in the $N = 1$ LL at very low temperatures and in the highest quality, single-subband samples exhibit FQH states at even-denominator fillings $\nu = 5/2$ and $7/2$ [22, 23]. In the traces shown in Fig. 1, we do not see any even-denominator states when $N = 1$, e.g., at $\nu = 7/2$ in region B where E_F is in the $S1\uparrow$ level. However, in the same sample, at higher densities ($n > 3.4 \times 10^{11} \text{ cm}^{-2}$) and at lower temperatures ($T < 30 \text{ mK}$), we do indeed observe a FQH state at $\nu = 7/2$ flanked by very weak $10/3$ and $11/3$ states when E_F lies in the $S1\uparrow$ level [24]. We defer a detailed discussion of the evolution of the even-denominator states in a two-subband system to future communication. Third, in the $N = 0$ LL, high-quality samples show strong higher-order, odd-denominator FQH states at composite Fermion filling factor sequences such as $2/5$, $3/7$, $4/9$, etc. [3]. We do observe a qualitatively similar behavior in our data when E_F is in a $N = 0$ LL. For example, in region A we see weak but clear minima at $\nu = 17/5$. Again, at higher densities and lower temperatures, such states become more developed [24].

In conclusion, the position of E_F is what determines the stability of odd-denominator FQH states at a given filling factor. When E_F lies in a ground-state ($N = 0$) LL, the odd-denominator FQH states are stable and strong. These FQH states also appear to be stable very near the crossing of two LLs, especially if the LLs have

parallel spins.

We acknowledge support through the NSF (DMR-0904117 and MRSEC DMR-0819860) for sample fabrication and characterization, and the DOE BES (DE-FG0200-ER45841) for measurements. We thank J. K. Jain and Z. Papić for illuminating discussions.

-
- [1] D. C. Tsui, H. L. Stormer, and A. C. Gossard, *Phys. Rev. Lett.*, **48**, 1559 (1982).
 - [2] R. B. Laughlin, *Phys. Rev. Lett.*, **50**, 1395 (1983).
 - [3] J. K. Jain, *Composite Fermions* (Cambridge University Press, New York, 2007).
 - [4] W. Pan, J.-S. Xia, V. Shvarts, D. E. Adams, H. L. Stormer, D. C. Tsui, L. N. Pfeiffer, K. W. Baldwin, and K. W. West, *Phys. Rev. Lett.*, **83**, 3530 (1999).
 - [5] C. Töke, M. R. Peterson, G. S. Jeon, and J. K. Jain, *Phys. Rev. B*, **72**, 125315 (2005).
 - [6] M. P. Lilly, K. B. Cooper, J. P. Eisenstein, L. N. Pfeiffer, and K. W. West, *Phys. Rev. Lett.*, **82**, 394 (1999).
 - [7] R. Du, D. Tsui, H. Stormer, L. Pfeiffer, K. Baldwin, and K. West, *Solid State Communications*, **109**, 389 (1999).
 - [8] G. Gervais, L. W. Engel, H. L. Stormer, D. C. Tsui, K. W. Baldwin, K. W. West, and L. N. Pfeiffer, *Phys. Rev. Lett.*, **93**, 266804 (2004).
 - [9] F. Haldane, *The quantum Hall effect*, edited by R. Prange and S. Girvin.
 - [10] A. H. MacDonald and S. M. Girvin, *Phys. Rev. B*, **33**, 4009 (1986).
 - [11] N. d'Ambrumenil and A. Reynolds, *Journal of Physics C: Solid State Physics*, **21**, 119 (1988).
 - [12] A. A. Koulakov, M. M. Fogler, and B. I. Shklovskii, *Phys. Rev. Lett.*, **76**, 499 (1996).
 - [13] R. Moessner and J. T. Chalker, *Phys. Rev. B*, **54**, 5006 (1996).
 - [14] Y. W. Suen, H. C. Manoharan, X. Ying, M. B. Santos, and M. Shayegan, *Phys. Rev. Lett.*, **72**, 3405 (1994).
 - [15] J. Shabani, T. Gokmen, Y. T. Chiu, and M. Shayegan, *Phys. Rev. Lett.*, **103**, 256802 (2009).
 - [16] K. Muraki, T. Saku, and Y. Hirayama, *Phys. Rev. Lett.*, **87**, 196801 (2001).
 - [17] K. Vakili, T. Gokmen, O. Gunawan, Y. P. Shkolnikov, E. P. De Poortere, and M. Shayegan, *Phys. Rev. Lett.*, **97**, 116803 (2006).
 - [18] Traces taken at higher values of Δ reveal that the $\nu = 7/3$ and $8/3$ states remain strong up to the $\nu = 3$ coincidence. Past this coincidence, the $7/3$ and $8/3$ states become weaker, consistent with the fact that E_F now lies in an excited LL (the $S1\uparrow$ level, see Fig. 2b).
 - [19] The $E_C + E_Z$ line going through region I does not correspond to a LL coincidence in this region; this should be evident from Fig. 2b diagram. The same is true about the $2E_C - E_Z$ line as it goes through region G.
 - [20] T. Jungwirth, S. P. Shukla, L. Smrčka, M. Shayegan, and A. H. MacDonald, *Phys. Rev. Lett.*, **81**, 2328 (1998).
 - [21] C. R. Dean, A. F. Young, P. Cadden-Zimansky, L. Wang, H. Ren, K. Watanabe, T. Taniguchi, P. Kim, J. Hone, and K. L. Shepard, "Multicomponent fractional quantum hall effect in graphene," (2010), arXiv:1010.1179.
 - [22] R. Willett, J. P. Eisenstein, H. L. Stormer, D. C. Tsui, A. C. Gossard, and J. H. English, *Phys. Rev. Lett.*, **59**,

- 1776 (1987).
- [23] W. Pan, J. S. Xia, H. L. Stormer, D. C. Tsui, C. Vicente, E. D. Adams, N. S. Sullivan, L. N. Pfeiffer, K. W. Baldwin, and K. W. West, Phys. Rev. B, **77**, 075307 (2008).
- [24] J. Shabani, Y. Liu, and M. Shayegan, Phys. Rev. Lett., **105**, 246805 (2010).